DOI: 10.1002/ejic.200501099

Alteration in the Binding Property of a Laterally Nonsymmetric Aza Cryptand toward Cu^{II}, Ag^{I}, and Tl^{I} Ions upon Derivatization with a Cyanomethyl Group

Debdas Ray[a] and Parimal K. Bharadwaj*[a]

Keywords: Cryptands / Coordination chemistry / Metal cryptate / Silver / Copper / Thallium

The laterally nonsymmetric aza cryptand $\mathbf{L_o}$ readily forms mononuclear inclusion complexes with metal ions like Cu^{II}, Ni^{II}, Ag^{I}, Tl^{I}, and so forth. However, when the secondary amines present in the three bridges are substituted by a cyanomethyl group to yield a new cryptand **L**, its metal-binding properties are drastically altered. Thus, while $\mathbf{L_o}$ binds Ag^{I} at the tren end, showing AgN_4 coordination, in **L**, the bridgehead nitrogen atoms are pulled inside to form a two-coordinate complex of Ag^{I} and none of the O or N atoms present in the three bridges are involved in coordination. This is probably the first example where the two bridgehead atoms are pulled inside to the maximum to bind the metal ion. Likewise, the Tl^{I} ion shows TlN_4 coordination with $\mathbf{L_o}$, while in **L** it is loosely bound at the tren end, showing TlN_3 coordination. Upon treatment with a Ag^{I} salt, the Tl^{I} can be replaced almost instantaneously. On the other hand, with copper(II) tetrafluoroborate salt in moist DMF, two of the cyanide groups in **L** are converted to carboxylic acid groups and bind the metal ion from outside. The Cu^{II} ion in this complex shows distorted octahedral coordination where the two O atoms from the two carboxylic acid groups and the two corresponding N atoms in the two bridges are bound equatorially. The two axial sites are occupied by the nearby bridgehead N atom and the O atom of a DMF molecule. All five complexes and the free ligands are characterized by spectroscopic and X-ray crystallographic studies.

Introduction

Macrobicyclic cryptands[1] possess several desirable properties, such as the topology of the donor atoms, binding-site rigidity, layer effects, and so forth, that determine stability, selectivity, and properties of their complexes with metal ions. One of the important factors in the formation of metal cryptates is the cryptand conformation equilibria. For cryptands with N bridgeheads, the principal conformers arise from different orientations of the lone pairs of the electrons on the bridgehead atoms.[2] Each lone pair may be oriented into the cavity (*endo*) or away from the cavity (*exo*). Therefore, it is easy to envision a minimum of three possible conformations for the nitrogen atoms as *exo-exo*, *exo-endo*, and *endo-endo*. The cryptand $\mathbf{L_o}$ (Figure 1) has a large cavity in which two distinct binding sites are separated by a hydrophobic spacer. The tren end (N_4 moiety) represents[1c,3] a suitable binding site for transition as well as main-group metal ions such as Ni^{II}, Cu^{II}, Zn^{II}, Pb^{II}, Ag^{I}, and so forth. The NO_3 moiety can be expected to be effective in binding harder cations. We were interested in observing any possible alteration in the coordinating ability of the cryptand when the donor ability of the nitrogen atoms was suppressed by attaching electron-withdrawing cyanomethyl groups to them (Figure 1). Tuning the stereoelectronic factors associated with the binding site has the ultimate aim of enforcing unusual coordination mode(s) on the metal ion besides potential applications associated with metal bind-

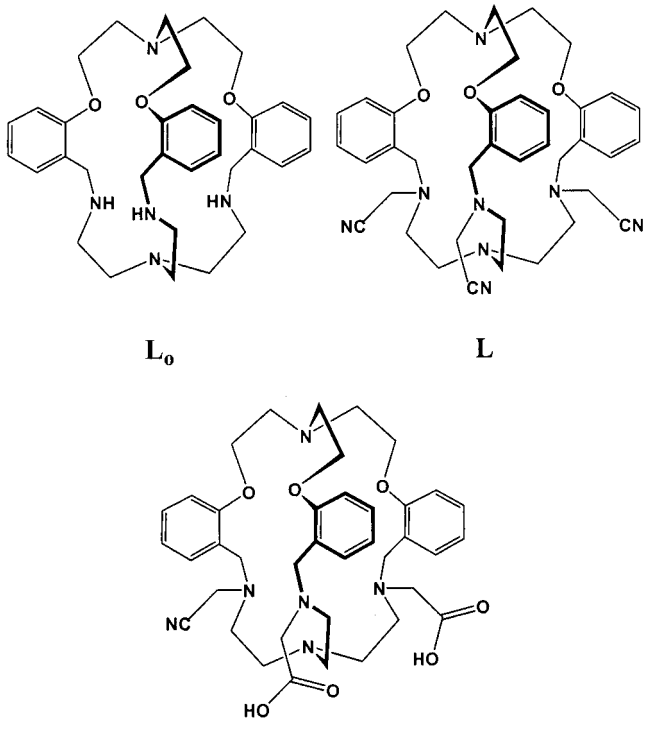

Figure 1. Schematic diagrams of cryptands $\mathbf{L_o}$, **L**, and **L**′.

[a] Department of Chemistry, Indian Institute of Technology, Kanpur 208016, India
E-mail: pkb@iitk.ac.in

ing.[4–6] In the present study, Cu^{II}, Ag^{I}, and Tl^{I} ions are used to probe the complexing ability of the cryptands.

Results and Discussion

The structure of $\mathbf{L_o}$ has an *endo-exo* conformation in which the distance between the bridgehead N atoms is 6.272(12) Å (Figure 2). A pseudo threefold axis passes through the bridgehead N atoms.

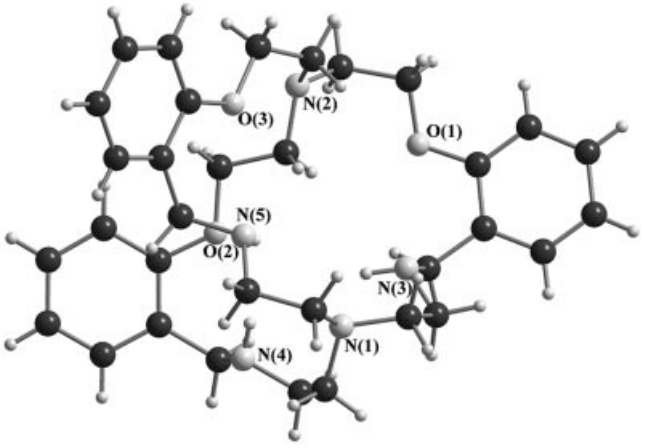

Figure 2. Perspective view of the cryptand $\mathbf{L_o}$.

For comparison, in the room-temperature structure of this cryptand,[7] the distance between the two bridgehead nitrogen atoms is 6.249(14) Å. The O···O and N···N nonbonding distances are also comparable between the two structures [$\mathbf{L_o}$ (LT) and $\mathbf{L_o}$ (RT)[7]]. Thus, temperature variation has little effect on cryptand conformation.

The asymmetric unit of **L** consists of a single strand of the cryptand and a water molecule. The nonbonding distances between two ethereal O atoms [4.72(1) Å] or two amino N atoms [4.29(1) Å] are the same because of crystallographically imposed symmetry. Therefore, in the solid state, the molecule has a threefold symmetry axis passing through the two bridgehead atoms. This cryptand has an *endo-endo* conformation in which the distance between the two bridgehead N atoms is 5.939(2) Å (Figure 3a). The shrinkage of the cryptand cavity relative to that of $\mathbf{L_o}$ may be due to a combination of delocalization of the electron density from the N atoms in the three bridges onto the cyanomethyl groups and the steric effects of these groups. The bond lengths and bond angles in the cryptand are within normal statistical errors. The ^{1}H NMR spectroscopic data of **L** also indicate threefold symmetry in the molecule in $CDCl_3$. An interesting feature of this structure is the presence of a triangular planar trimeric water cluster, which shows positional disorder and can be described as two sets of triangular planar water clusters. Six cryptand molecules surround the water cluster (Figure 3b) where each water molecule shows a weak C–H···O hydrogen-bonding interaction [d(H···O) = 2.340(16) Å] with the nearest benzene group. The existence of aromatic C–H···O hydrogen bonds has been inferred from several theoretical[8] as well as experimental[9] studies in different organic crystal lattices.[10]

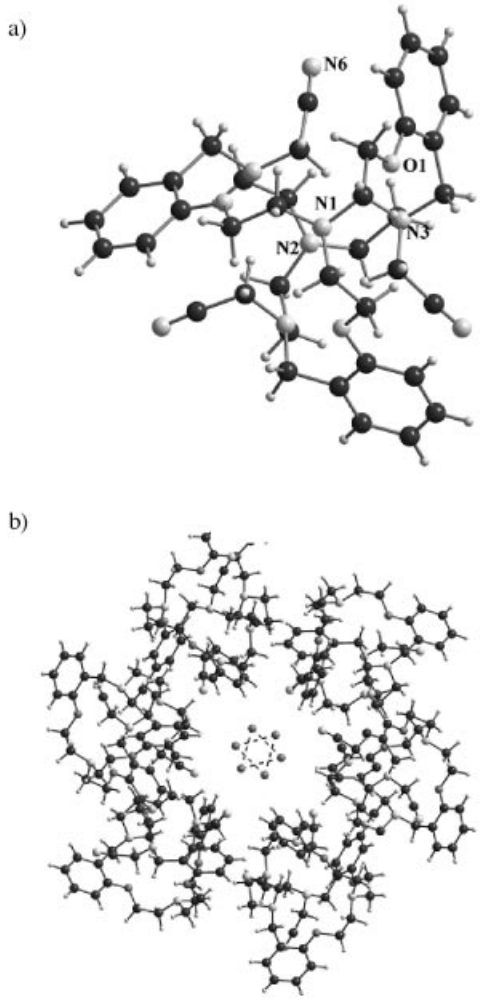

Figure 3. (a) Cryptand **L** viewed approximately along the threefold axis. (b) Packing of six **L** molecules around a cyclic water trimer. Two trimers are shown illustrating positional disorder.

The structure of complex **1** consists of an $[AgL]^+$cation and a nitrate anion. One molecule of methanol is also present in the lattice. The Ag^{I} ion is bonded to four nitrogen atoms at the tren end of the cryptand and is positioned 0.71 Å above the plane described by three amino N atoms in the direction away from the bridgehead N atom (Figure 4). Thus, the coordination geometry is very distorted; all four nitrogen atoms are on one side of the metal ion. Such distorted geometry for an Ag^{I} cryptate was reported[11] earlier. The bond lengths and angles involving the metal ion are similar to those found[11–13] in other Ag cryptates. The metal ion is more than 2.9(1) Å away from the ethereal oxygen atoms and so is considered to be nonbonded. The separation between the two bridgehead N atoms is found to be 5.983(7) Å, which is slightly less than the distance found in $\mathbf{L_o}$ (Table 1). The other N···N and O···O nonbonding distances do not vary appreciably upon metal binding, which means that the cryptand is mostly preorganized.

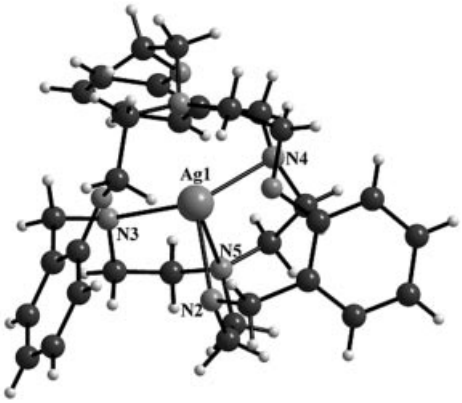

Figure 4. View of the Ag^{I} ion bound at the tren end of the cavity in $\mathbf{L_o}$.

The structure of **2** shows that the Ag^{I} ion is bonded inside the cavity of **L** in an unprecedented fashion (Figure 5). Here, either the electron-withdrawing groups attached to the amino groups make the lone pair unavailable for metal binding or the methylene group of the $-CH_2CN$ moiety near the aromatic group might prevent closer interaction between the amino nitrogen atom and a metal ion. However, the Ag^{I} ion shows dicoordination, binding the two bridgehead N atoms at Ag–N distances of 2.325(8) and 2.388(8) Å and at an N–Ag–N angle of 167.7(10)°. Few two-coordinate Ag^{I} complexes are known[14] in the literature with similar bond lengths and angles. The distance between the metal ion and any other N atoms in the three bridges is 2.82(6) Å or more, while the distance between the metal ion and an ethereal O atom is at least 2.63(5) Å; the metal ion may be considered to be semibonded to the oxygen atom. The bond lengths and bond angles of the cryptand moiety are within normal statistical errors. The two bridgehead N atoms are significantly pulled inside by the Ag^{I} ion; the distance between them is 4.687(15) Å. A water dimer is also present in the lattice, which is hydrogen-bonded to the nitrate anion [O···Ow1 3.019(12) Å].

The unsubstituted cryptand $\mathbf{L_o}$ forms an inclusion complex with Tl^{I} (complex **3**) in which the metal ion occupies a site at the tren end. The Tl^{I} ion is in a "4+3" coordination environment with four normal[15] Tl–N bonds [2.788(8)–2.869(9) Å] and three long interactions [3.07(9)–3.14(9) Å]; the ethereal O atoms are in the cryptand side arms (Figure 6). However, the Tl–N bond lengths are at the long end of the range for Tl–N distances, and therefore are ionic in character,[15a,15b] although Tl–O bond lengths are comparable to literature values.[15f] In complex **4**, on the other hand, Tl^{I} exhibits "3+5" coordination (Figure 7), which comprises three normal Tl–N bonds and five long interactions with the remaining donor atoms (Table 1). The Tl–N bond lengths are significantly increased relative to the values obtained for **3**. Hence, even though the Tl^{I} ion is positioned at the tren end and bonds to the N atoms attached to the cyanomethyl groups, the bonding is weak and ionic in character. In either **3** or **4**, the metal ion is symmetrically bonded to N and O donors and the lone pair on Tl^{I} does

Table 1. Selected bond lengths [Å], angles [°], and nonbonded distances [Å].

$\mathbf{L_o}$		**L**	
N(3)···N(4)	4.067	N(3)···N(3′)	4.298
N(3)···N(5)	4.417	N(1)···N(2)	5.936
N(4)···N(5)	3.547	O(1)···O(1′)	4.731
N(1)···N(2)	6.272		
O(1)···O(2)	4.855		
O(1)···O(3)	5.380		
O(2)···O(3)	3.967		
1		**2**	
Ag–N(3)	2.425(5)	Ag–N(2)	2.326(8)
Ag–N(4)	2.402(5)	Ag–N(1)	2.388(8)
Ag–N(5)	2.569(5)		
Ag–N(2)	2.465(5)		
N(3)–Ag–N(4)	117.63(17)	N(2)–Ag–N(1)	167.71(10)
N(3)–Ag–N(5)	73.51(17)		
N(4)–Ag–N(5)	73.82 (15)		
N(3)–Ag–N(2)	100.54(15)		
N(4)–Ag–N(2)	117.93(15)		
N(5)–Ag–N(2)	72.75(14)		
N(3)···N(4)	4.130	N(3)···N(4)	5.058
N(3)···N(5)	2.990	N(3)···N(5)	5.684
N(4)···N(5)	2.988	N(4)···N(5)	4.387
N(1)···N(2)	4.903	N(1)···N(2)	4.687
O(1)···O(2)	3.999	O(1)···O(2)	4.662
O(1)···O(3)	4.357	O(1)···O(3)	4.878
O(2)···O(3)	4.210	O(2)···O(3)	4.667
	3		**4**
Tl–N(2)	2.869(9)	Tl–N(2)	2.902(9)
Tl–N(3)	2.788(5)	Tl–N(3)	3.013(5)
Tl–N(4)	2.865(8)	Tl–N(4)	2.907(5)
Tl–N(5)	2.848(9)	Tl–N(5)	2.834(7)
Tl–O(1)	3.077(9)	Tl–O(1)	3.099(5)
Tl–O(2)	3.084(5)	Tl–O(2)	3.182(5)
Tl–O(3)	3.144(9)	Tl–O(3)	3.010(8)
N(3)–Tl–(N4)	95.59(15)	N(3)–Tl–N(4)	107.65(7)
N(3)–Tl–N(5)	116.11(15)	N(3)–Tl–N(5)	99.86(8)
N(4)–Tl–N(5)	95.42(15)	N(4)–Tl–N(5)	101.06(8)
N(3)–Tl–N(2)	65.42(15)	N(3)–Tl–N(2)	62.98(7)
N(4)–Tl–N(2)	62.96(14)	N(4)–Tl–N(2)	65.40(8)
N(5)–Tl–N(2)	64.93(14)	N(5)–Tl–N(2)	65.44(8)
N(3)···N(4)	4.187	N(3)–N(4)	4.779
N(3)···N(5)	4.782	N(3)···N(5)	4.476
N(4)···N(5)	4.226	N(4)···N(5)	4.432
N(1)···N(2)	6.073	N(1)···N(2)	6.007
O(1)···O(2)	4.907	O(1)···O(2)	4.733
O(1)···O(3)	4.284	O(1)···O(3)	4.522
O(2)···O(3)	4.395	O(2)···O(3)	4.544
5			
Cu–O(8)	1.980		
Cu–O(4)	1.985		
Cu–N(2)	2.056		
Cu–N(4)	2.059		
Cu–O(6)	2.330		
Cu–N(3)	2.349		
O(8)–Cu–O(4)	95.24(2)		
O(8)–Cu–N(2)	170.71(2)		
O(4)–Cu–N(2)	91.47(2)		
O(8)–Cu–N(4)	87.66(2)		
O(4)–Cu–N(4)	164.75(3)		
N(2)–Cu–N(4)	87.54(2)		
O(8)–Cu–O(6)	90.11(1)		
O(4)–Cu–O(6)	89.26(2)		
N(2)–Cu–O(6)	96.39(2)		
N(4)–Cu–O(6)	75.74(1)		
O(8)–Cu–N(3)	90.14(1)		
O(4)–Cu–N(3)	80.12(1)		
N(2)–Cu–N(3)	84.69(2)		
N(4)–Cu–N(3)	114.90(2)		
O(6)–Cu–N(3)	169.36(2)		
N(3)···N(4)	3.719		
N(3)···N(5)	5.693		
N(4)···N(5)	5.515		
N(1)···N(2)	4.653		
O(1)···O(2)	4.505		
O(1)···O(3)	5.482		
O(2)···O(3)	5.794		

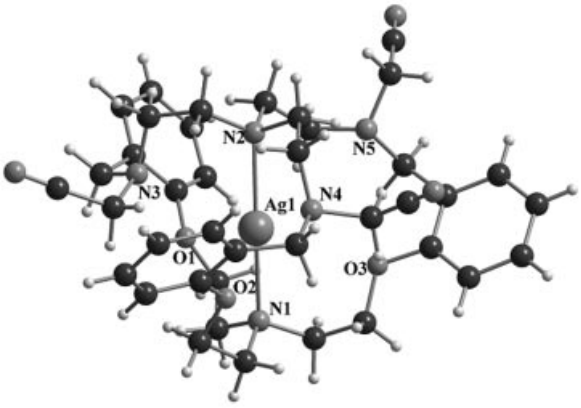

Figure 5. View of the Ag^{I} ion bound to the two bridgehead N atoms in **L**. H atoms are omitted for clarity.

not seem to be stereochemically active.[16] When an equivalent amount of $AgNO_3$ is added to an acetonitrile solution of either **2** or **3**, the Tl^{I} ion is quantitatively replaced by Ag^{I}-forming crystals of **1** or **2** overnight.

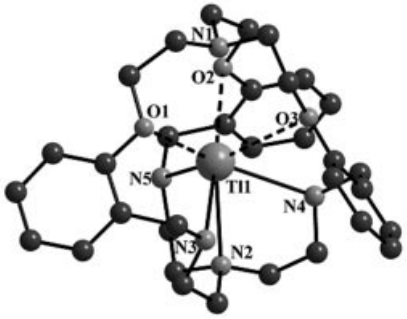

Figure 6. Perspective view of **3** showing the Tl^{I} ion bound at the tren end of $\mathbf{L_o}$.

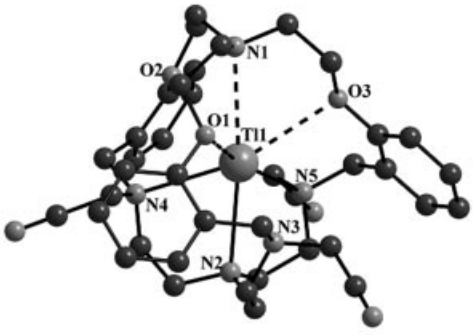

Figure 7. View of **4** showing the Tl^{I} ion bound to three N atoms at the tren end of **L**.

The structure of **5** consists of discrete $[Cu(\mathbf{L}')(DMF)]^{2+}$ cations (Figure 8) and BF_4^- anions. One DMF molecule is also present in the lattice. This structure reveals that two out of three cyano groups are hydrolyzed to carboxylic acid groups and bind a Cu^{II} ion from outside at the tren end of the cavity. The H atoms bonded to the carboxylic acid groups could be easily found in the difference map. We speculate that Cu^{II} initially binds the cryptand outside the cavity and activates the cyano group, which is then attacked by H_2O. Only two cyano groups are activated, as the third one is far away from the metal ion. However, the UV/Vis data for the hydrolysis of the cyano group taken at different intervals were not informative. Many metal-mediated processes of cyano group hydrolysis are known in the literature.[17] As a result of hydrolysis of the two cyano groups to carboxylic acid groups, the corresponding N atoms in the two bridges are no longer electron-deficient and bind the Cu^{II} ion along with the two O atoms from the two carboxylic acid groups equatorially. The two axial sites are occupied by the nearby bridgehead N atom and the O atom of a DMF molecule, forming a distorted octahedral coordination geometry (Table 1) around the metal ion. The three N donors from the cryptand are inverted, their lone pairs being directed toward the metal ion, and the cryptand adopts an *exo-endo* conformation. The bond lengths and angles in the cryptand moiety are within normal statistical error, while those involving the metal ion (Table 1) are similar[18] to other Cu^{II} cryptates.

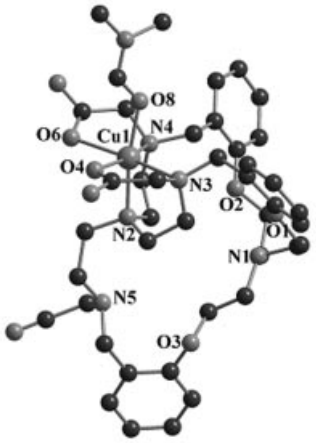

Figure 8. A view of the Cu^{II} ion bound outside the cryptand cavity. Lattice DMF and H atoms bonded to C are omitted for clarity.

In the UV/Vis spectral studies, **5** shows a broad ligand-field band at 685 nm and a charge-transfer band at 325 nm, with molar extinction coefficients of 35 and 600 $cm^2 \cdot mol^{-1}$, respectively. The effective magnetic moment value (μ_{eff}/μ_B) for **3** after diamagnetic correction is found to be 2.02 at 293 K, which is consistent[19] with the discrete, mononuclear formulation of the complex. EPR spectral studies were carried out in the solid state and in DMF solution at 295 and 77 K. In the solid state at 295 K, a broad signal with g_{av} = 2.09 is observed. The signal sharpens at 80 K without revealing any fine structure. In DMF solution at 80 K, an axial spectrum is obtained with $g_{\|}$ = 2.21, $g_{\perp}$ = 2.08, and $A_{\|} = 148 \times 10^{-4}$ cm^{-1}.

Conclusion

We show here that, although the unsubstituted cryptand binds an Ag^{I} ion inside the cavity without significant change of the cryptand conformation, it behaves very dif-

ferently when electron-withdrawing groups are attached to the amino nitrogen atoms in the three bridges. The amino nitrogen atoms lose their ability to bind Ag^{I}. Instead, the metal ion binds the two bridgehead N atoms, which is unprecedented. On the other hand, the Tl^{I} ion forms an inclusion complex with $\mathbf{L_o}$, in which the metal ion occupies the tren end of the cavity and is ligated by all four N atoms. With **L**, Tl^{I} still occupies the same end of the cavity but is loosely bound to three N atoms and can be readily replaced by Ag^{I}. In the case of Cu^{II}, two of the cyano groups are hydrolyzed to carboxylic acid groups at room temperature. This change restores the donor ability of the amino N atoms and the cryptand binds a Cu^{II} ion outside the cavity in a distorted octahedral fashion. We are presently probing whether it is possible to have mixed-metal complexes with this and other related cryptands.

Experimental Section

Materials: All reagent-grade chemicals were used without purification unless otherwise specified. The metal salts, bromoacetonitrile, and tris(2-aminoethyl)amine were obtained from Aldrich. Triethanolamine, salicylaldehyde, sodium borohydride, sodium hydroxide, anhydrous sodium sulfate, potassium carbonate, thionyl chloride, and solvents were received from S. D. Fine Chemicals (India). Thionyl chloride and all the solvents were freshly distilled prior to use, and all the reactions were carried out under N_2.

Physical Measurements: Spectroscopic data were collected as follows: IR (KBr disk, 400–4000 cm^{-1}) Perkin–Elmer Model 1320; ^1H NMR ([D_6]DMSO, TMS) JEOL JNM-LA400 FT, 400 MHz. FAB MS (positive ion, argon as the FAB gas, 6 kV, 10 mA, 10 kV accelerating voltage) JEOL SX 102/DA-6000. Magnetic susceptibility measurements were made by using a Cahn Faraday Balance with [$CoHg(SCN)_4$] as the standard and applying diamagnetic corrections as described earlier.[18] The EPR spectrum for complex **3** was recorded at X-band frequency with a BRUKER 300E automatic spectrometer at 298 and 80 K. Melting points were determined with an electrical melting point apparatus by PERFIT, India, and were uncorrected. Elemental analyses were obtained from CDRI, Lucknow.

Synthesis

Cryptand $\mathbf{L_o}$: It was synthesized as reported[7] earlier. Single crystals suitable for X-ray crystallography were grown by slow concentration of an acetonitrile solution at room temperature.

Cryptand L: Cryptand $\mathbf{L_o}$ (1 g, 1.78 mmol) was added to a suspension of anhydrous potassium carbonate (0.86 g, 6.25 mmol) in dry acetonitrile (100 mL). The solution was stirred at 30 °C. After 30 min, bromoacetonitrile (0.42 mL, 6.25 mmol) was added to the stirred solution. The mixture was stirred at 30 °C for 24 h, and the solvent was removed completely in a rotary evaporator. The black solid that remained was shaken with water and then extracted with chloroform (3 × 50 mL). The chloroform layer, after being decolorized with activated charcoal and dried with anhydrous sodium sulfate, was concentrated completely to yield a yellowish white solid as the desired product. It was purified further by crystallization from dichloromethane to obtain colorless crystals in the form of rectangular parallelepipeds. Yield ca. 85% (1.02 g). M.p. 160 °C. ^1H NMR (400 MHz, $CDCl_3$, 25 °C, TMS): aliphatic: δ = 2.65 (dd, J = 22.12, 5.4 Hz, 12 H), 3.18 (t, J = 5.32 Hz, 6 H), 3.46 (s, 6 H), 3.52 (s, 6 H), 4.06 (t, J = 5.12 Hz, 6 H); aromatic: δ = 6.78 (d, J = 8.04 Hz, 3 H), 6.93 (t, J = 7.32 Hz, 3 H), 7.14–7.26 (m, 6 H) ppm. FAB-MS: m/z (%) = 677 $[\mathbf{L}]^+$ (100). $C_{39}H_{48}N_8O_3$ (678): calcd. C 69.21, H 7.15, N 16.56; found C 69.28, H 7.21, N 16.67.

$[Ag(L_o)]\cdot(NO_3)\cdot CH_3OH$ (1): Cryptand $\mathbf{L_o}$ (0.56 g, 1 mmol) in dry methanol (5 mL) was added at once to an acetonitrile solution (5 mL) of $AgNO_3$ (0.17 g, 1 mmol) at room temperature in the dark. The light brown solution formed was filtered and the filtrate stored in the dark for crystallization. Colorless X-ray quality crystals in the form of rectangular parallelepipeds appeared in about 2 d. Yield ca. 35% (0.67 g). $C_{34}H_{49}AgN_6O_7$ (761.66): calcd. C 53.61, H 6.48, N 11.034; found C 53.43, H 6.52, N 10.98.

$[Ag(L)]\cdot(NO_3)\cdot 2H_2O$ (2): Cryptand **L** (0.68 g, 1 mmol) in dry acetonitrile (5 mL) was added to an acetonitrile solution (5 mL) of $AgNO_3$ (0.17 g; 1 mmol) at room temperature in the dark. The light brown solution was filtered and the filtrate kept for crystallization. Colorless, X-ray-quality, square crystals appeared in 3 d. Yield ca. 55% (0.47 g). $C_{39}H_{52}AgN_9O_8$ (882.75): calcd. C 53.06, H 5.93, N 14.28; found C 52.92, H 5.90, N 14.13.

$[Tl(L_o)](CH_3OH)(ClO_4)$ (3): The cryptand $\mathbf{L_o}$ (0.56 g, 1 mmol) dissolved in dry methanol (5 mL) was added all at once to a CH_3CN solution (3 mL) of $Tl(ClO_4)\cdot xH_2O$ (0.36 g, 1.2 mmol) at room temperature in the dark. A brown solution was obtained that was filtered, and the filtrate was stored at room temperature while the solvent evaporated. White X-ray-quality rectangular crystals of **4** appeared in about 2 d. Yield ca. 50% (0.45 g). $C_{34}H_{49}Cl_1N_5O_8Tl$ (895.62): calcd. C 45.60, H 5.51, N 7.82; found C 45.78, H 5.38, N 7.40.

$[Tl(L)](H_2O)(ClO_4)$ (4): Cryptand **L** (0.68 g; 1 mmol) in dry acetonitrile (5 mL) was added to an acetonitrile solution (5 mL) of $Tl(ClO_4)\cdot xH_2O$ (0.36 g, 1.2 mmol) at room temperature in the dark. The light brown solution was filtered and the filtrate kept for crystallization. Colorless, X-ray-quality, square crystals appeared in 3 d. Yield ca. 55% (0.55 g). $C_{39}H_{50}Cl_1N_8O_8Tl$ (998.70): calcd. C 46.90, H 5.05, N 11.22; found C 49.75, H 5.11, N 11.09.

$[Cu(L')(DMF)]\cdot(BF_4)_2\cdot DMF$ (5): Cryptand **L** (0.68 g, 1 mmol), dissolved in dry DMF (3 mL) was added all at once to a DMF solution (3 mL) of $Cu(BF_4)_2\cdot xH_2O$ (0.23 g, 1.2 mmol) at room temperature. A blue-green solution was obtained that was filtered and the filtrate was stored at room temperature while the solvent evaporated. Blue-green, X-ray-quality, rectangular crystals of **5** appeared in about 7 d. Yield ca. 50% (0.55 g). $C_{45}H_{64}CuN_8O_9(BF_4)_2$ (1098.2): calcd. C 49.21, H 5.87, N 10.20; found C 49.44, H 5.99, N 10.38.

X-ray Structural Studies: Single-crystal X-ray data were collected at 100 K with a Bruker SMART APEX CCD diffractometer using graphite-monochromated Mo-K_α radiation (λ = 0.71073 Å). The linear absorption coefficients, scattering factors for the atoms, and the anomalous dispersion corrections were taken from the International Tables for X-ray Crystallography. Data integration and reduction were processed with the SAINT[20] software. The structure was solved by direct methods using SHELXTL and was refined on F^2 by full-matrix least-squares techniques using the SHELXL-97 program[21] package. All non-hydrogen atoms were refined anisotropically except C(33) of compound **1**, which was refined isotropically. All hydrogen atoms were located in successive difference Fourier maps and they were treated as riding atoms by using SHELXL default parameters. The crystal data for the structures are collected in Tables 1 and 2. CCDC-290844 to -290850 contain the supplementary crystallographic data for this paper. These data can be obtained free of charge from The Cambridge Crystallographic Data Centre via www.ccdc.ac.uk/data_request/cif.

Table 2. Crystal data and structure refinement for $\mathbf{L_o}$, **L**, **1**–**5**.

	$\mathbf{L_o}$	**L**	**1**	**2**	**3**	**4**	**5**
Empirical formula	$C_{33}H_{45}NO_3$	$C_{13}H_{14}NO_2$	$C_{34}H_{48}AgN_6O_7$	$C_{39}H_{48}AgN_9O_8$	$C_{34}H_{49}ClN_5O_7Tl$	$C_{39}H_{50}ClN_5O_8Tl$	$C_{45}H_{64}B_2CuF_9N_8O_{10}$
Formula mass	559.74	258.28	760.65	878.73	879.59	998.31	1133.20
T [K]	100	100	100	100	100	100	100
Radiation	Mo-K_α	Mo-K_α	Mo-K_α	Mo-K_α	Mo-K_α	Mo-K_α	Mo-K_α
Wavelength [Å]	0.71073	0.71073	0.71073	0.71073	0.71073	0.71073	0.71073
Crystal system	triclinic	cubic	triclinic	monoclinic	triclinic	monoclinic	triclinic
Space group	$P\bar{1}$	Pa-3	$P\bar{1}$	$P2_1/n$	$P\bar{1}$	$P2_1/n$	$P\bar{1}$
a [Å]	10.114(5)	19.4675(6)	9.6638(8)	11.135(5)	9.869(5)	11.865(5)	13.896(5)
b [Å]	11.823(5)	19.4675(6)	12.6337(10)	19.080(5)	13.036(5)	19.239(5)	16.210(5)
c [Å]	13.297(5)	19.4675(6)	13.8277(11)	19.250(5)	14.200(5)	18.268(5)	16.396(5)
α [°]	106.953(5)	90	86.2680(10)	90	90.118(5)	90	107.285(5)
β [°]	91.408(5)	90	88.076(2)	105.182(5)	101.290(5)	103.036(5)	101.442(5)
γ [°]	91.032(5)	90	86.9580(10)	90	99.934(5)	90	112.632(5)
V [Å^3]	1519.9(11)	7377.9(4)	1681.5(2)	3947(2)	1763.4(14)	4063(2)	3043.1(17)
Z	2	24	2	4	2	4	2
$\rho_{calcd.}$ [mg·m^{-3}]	1.223	1.248	1.502	1.479	1.687	1.633	1.199
μ [mm^{-1}]	0.079	0.083	0.657	0.575	4.713	4.103	0.435
F (000)[a]	604	2960	794	1824	900	2008	1146
Reflections collected	9804	47225	11217	26186	11670	26621	20385
Independent reflections	7158	3065	7983	9756	8354	9905	14479
Goof	1.029	1.118	1.067	0.849	1.017	1.033	1.043
Final R[b] indices							
R_1	0.0652	0.0759	0.0597	0.0577	0.0497	0.0331	0.0718
wR_2	0.1482	0.1727	0.1428	0.1413	0.1296	0.0793	0.2219
R indices							
R_1	0.1280	0.0962	0.0689	0.0750	0.0542	0.0439	0.0927
(all) wR_2	0.1746	0.1837	0.1486	0.1542	0.1327	0.0838	0.2072

[a] Refinement method: full-matrix least squares on F^2. [b] $R = \Sigma||F_o| - |F_c||/|F_o|$; $wR_2 = \Sigma[w(F_o^2 - F_c^2)^2]/\Sigma[w(F_o^2)^2]^{1/2}$.

Acknowledgments

Financial support from the Department of Science and Technology, New Delhi, India (grant no. SR/S5/NM-38/2003 to P. K. B.) and an SRF (CSIR, New Delhi) to D. R. are gratefully acknowledged.

[1] a) J.-M. Lehn, *Supramolecular Chemistry – Concepts and Perspectives*, VCH Publishers, Weinheim, Germany, **1995**; b) J. Nelson, J. V. McKee, G. Morgan, *Prog. Inorg. Chem.* **1998**, *47*, 167–316; c) B. Sarkar, P. Mukhopadhyay, P. K. Bharadwaj, *Coord. Chem. Rev.* **2003**, *236*, 1–13.
[2] R. Geue, S. H. Jacobson, R. Pizer, *J. Am. Chem. Soc.* **1986**, *108*, 1150–1155.
[3] P. K. Bharadwaj, *Prog. Inorg. Chem.* **2003**, *51*, 251–331.
[4] P. Mukhopadhyay, B. Sarkar, P. K. Bharadwaj, K. Nättinen, K. Rissanen, *Inorg. Chem.* **2003**, *42*, 4955–4960.
[5] a) P. Ghosh, P. K. Bharadwaj, J. Roy, S. Ghosh, *J. Am. Chem. Soc.* **1997**, *119*, 11903–11909; b) P. Mukhopadhyay, P. K. Bharadwaj, G. Savitha, A. Krishnan, P. K. Das, *Chem. Commun.* **2000**, 1815–1816.
[6] B. P. Bag, P. K. Bharadwaj, *Inorg. Chem.* **2004**, *43*, 4626–4630.
[7] D. K. Chand, K. Ragunathan, P. K. Bharadwaj, *J. Org. Chem.* **1996**, *61*, 1169–1171.
[8] S. Scheiner, *Hydrogen Bonding: A Theoretical Perspective*, Oxford University Press, New York, **1997**.
[9] H. Matsuura, H. Yoshida, M. Hieda, S. Yamanaka, T. Harada, K. Shin-ya, K. Ohno, *J. Am. Chem. Soc.* **2003**, *125*, 13910–13911.
[10] R. Thaimattam, F. Xue, J. A. R. P. Sarma, T. C. W. Mak, G. R. Desiraju, *J. Am. Chem. Soc.* **2001**, *123*, 4432–4445.
[11] O. W. Howarth, G. G. Morgan, V. McKee, J. Nelson, *J. Chem. Soc., Dalton Trans.* **1999**, 2097–2102.
[12] J. de Mendoza, E. Mesa, J.-C. Rodriguez-Ubis, P. Vàzquez, F. Vögtle, P.-M. Windscheif, K. Rissanen, J.-M. Lehn, D. Lilienbaum, R. Ziessel, *Angew. Chem. Int. Ed. Engl.* **1991**, *30*, 1331–1333.
[13] T. Sato, A. Suziki, K. Sakai, T. Tsubomura, *Bull. Chem. Soc. Jpn.* **1996**, *69*, 379–388.
[14] a) P. I. Richards, A. Steiner, *Inorg. Chem.* **2004**, *43*, 2810–2817; b) N. Schultheiss, D. R. Powell, E. Bosch, *Inorg. Chem.* **2003**, *42*, 8886–8890; c) R. R. Fenton, P. C. Junk, R. Gauci, L. F. Lindoy, R. C. Luckay, G. V. Meehan, J. R. Price, P. Turner, G. Wei, *J. Chem. Soc., Dalton Trans.* **2002**, 2185–2193.
[15] a) H. V. R. Dias, S. Singh, T. R. Cundari, *Angew. Chem. Int. Ed.* **2005**, *44*, 4907–4910; b) O. W. Howarth, J. Nelson, V. Mckee, *Chem. Commun.* **2000**, 21–22; c) B. H. Hamilton, C. J. Ziegler, *Inorg. Chem.* **2004**, *43*, 4272–4277; d) E. Craven, E. Mutlu, D. Lundberg, S. Temizdemir, S. Dechert, H. Brombacher, C. Janiak, *Polyhedron* **2002**, *21*, 553–562; e) A. J. Amoroso, J. C. Jeffery, P. J. Jones, J. A. McCleverty, E. Psillakis, M. D. Ward, *J. Chem. Soc., Chem. Commun.* **1995**, 1175–1176; f) P. L. Jones, K. L. V. Mann, J. C. Jeffery, J. A. McCleverty, M. D. Ward, *Polyhedron* **1997**, *16*, 2435–2440.
[16] A.-V. Mudring, F. Rieger, *Inorg. Chem.* **2005**, *44*, 6240–6243.
[17] V. Yu. Kukushkin, A. J. L. Pombeiro, *Chem. Rev.* **2002**, *102*, 1771–1802.
[18] D. K. Chand, P. K. Bharadwaj, *Inorg. Chem.* **1996**, *35*, 3380–3387.
[19] F. A. Cotton, G. Wilkinson, *Advanced Inorganic Chemistry*, 5th ed., Wiley, New York, **1988**.
[20] SAINT+, 6.02ed., Bruker AXS, Madison, WI, **1999**.
[21] G. M. Sheldrick, *SHELXTL™ Reference Manual*, version 5.1, Bruker AXS, Madison, WI, **1997**.

Received: December 7, 2005
Published Online: March 1, 2006

